



## UvA-DARE (Digital Academic Repository)

### Aspects of photodetection in cervical and ovarian neoplasia

Aalders, M.C.G.

**Publication date**  
2001

[Link to publication](#)

#### **Citation for published version (APA):**

Aalders, M. C. G. (2001). *Aspects of photodetection in cervical and ovarian neoplasia*. [Thesis, fully internal, Universiteit van Amsterdam].

#### **General rights**

It is not permitted to download or to forward/distribute the text or part of it without the consent of the author(s) and/or copyright holder(s), other than for strictly personal, individual use, unless the work is under an open content license (like Creative Commons).

#### **Disclaimer/Complaints regulations**

If you believe that digital publication of certain material infringes any of your rights or (privacy) interests, please let the Library know, stating your reasons. In case of a legitimate complaint, the Library will make the material inaccessible and/or remove it from the website. Please Ask the Library: <https://uba.uva.nl/en/contact>, or a letter to: Library of the University of Amsterdam, Secretariat, P.O. Box 19185, 1000 GD Amsterdam, The Netherlands. You will be contacted as soon as possible.

## **Chapter 7**

# **Double Ratio fluorescence imaging for the detection of early superficial cancers**

**Design, construction and performance of a clinical prototype**

Arjen Bogaards, Maurice Aalders, Armand Jongen, Erwin Dekker, Dick Sterenberg.

*Review of Scientific Instruments*, in Press, 2001.

## **Abstract**

We developed a fluorescence imaging device for the detection of superficial cancer based on the Double Ratio technique. In practical use this device resembles an operation microscope and can be used in a clinical environment. This device acquires 4 different fluorescence images excited at two wavelengths and detected at two wavelengths. From these images it calculates, displays and stores Double Ratio images at a maximum speed of 1Hz. The Double Ratio image gives the distribution of the fluorophore amount present in tissue and is not affected by local variations in tissue optics, i.e. tissue absorption and tissue scattering. The validity of the technique was confirmed here by *ex vivo* tissue equivalent phantom experiments using hematoporphyrin and *in vivo* experiments on normal pigmented moles on Caucasian human skin using 5-aminolevulinic acid induced protoporphyrin IX.

## Introduction

Early (pre)cancerous lesions are often hard to find under white light illumination. The medical community is searching for new non-invasive methods to detect these lesions, which often start in the epithelial layer up to a few hundred micrometers below the tissue surface. Fluorescence imaging is an upcoming non-invasive optical technique that produces *in vivo* images with information of these first few hundred micrometers. The interest of research groups<sup>1,2</sup>, the investments of various companies like Karl Storz GmbH. & Co. and Xillix Technologies Corp., in combination with recent promising clinical trials<sup>3-8</sup>, demonstrate the potential of this technique. In this paper we introduce a new fluorescence imaging device, which may provide diagnostic information about tissue in addition to that offered by currently available fluorescence imaging techniques.

Various approaches are currently under investigation for *in vivo* fluorescence imaging. Some techniques use fluorophores which are naturally present in the tissue, assuming differences in fluorophore content in normal and cancerous tissue<sup>9</sup>. Other techniques are based on administration of tumor localizing fluorescent drugs to enhance fluorescence contrast<sup>10</sup>. Here background fluorescence of natural tissue fluorophores biases the measurement and can be considered an artifact. Using two excitation wavelengths allows subtraction of this background fluorescence<sup>11</sup>. Detecting the fluorescence at two wavelengths allows a fluorescence measurement relative to a background<sup>12</sup>. Algorithms that are based on multiple excitation and detection wavelengths are also used to optimize contrast between normal and cancerous tissue<sup>13</sup>. Some of these methods are successful in specific medical fields, nevertheless, the measured fluorescence signal is influenced by factors which may not be directly related to (pre)malignancy. Factors like spatial variation in natural tissue fluorescence, geometry, variations in excitation fluence, tissue color and tissue scattering may seriously limit the reliability of fluorescence diagnosis<sup>14</sup>.

Attempting to avoid these limitations Sinaasappel and Sterenborg developed the Double Ratio (DR) fluorescence imaging technique<sup>15</sup>. This technique aims to detect a tumor localizing fluorophore, where the DR image gives the distribution of the fluorophore amount present in tissue. In theory, this technique corrects for variations in natural tissue fluorescence, geometry and excitation fluence. Most important, the DR technique also corrects for spatial variations in tissue optics, i.e. tissue absorption and tissue scattering. This was confirmed earlier by *in vitro* and *in vivo* point measurement experiments<sup>15,16</sup>. With these unique and useful correction properties, DR imaging may provide diagnostic

information in addition to currently available fluorescence imaging methods.

In this paper we describe a DR fluorescence imaging device. First we briefly explain the fundamentals on which the imaging technique is based, followed by a description of the prototype design and construction. Finally, the dependence on tissue optics is investigated by *ex vivo* experiments on tissue equivalent phantoms and *in vivo* experiments on human moles.

## Materials and methods

The double ratio technique is based on the acquisition of 4 fluorescence signals. Sinaasappel and Sterenberg defined the double ratio as<sup>15</sup>:

$$\text{Double Ratio} \propto \frac{F_{i,t} F_{j,r}}{F_{j,t} F_{i,r}} \quad (1)$$

Where F stands for the 4 fluorescence signals, the indices i and j refer to different excitation wavelengths and the indices t and r to different detection wavelengths.  $F_{i,t}/F_{j,t}$  is the 'target ratio' of the 'target fluorophore', i.e. the tumor localizing fluorescent drug and  $F_{i,r}/F_{j,r}$  is the 'reference ratio' of the 'reference fluorophore', i.e. the natural tissue fluorescence. The reference ratio is assumed independent of the 'target fluorophore', while the target ratio is assumed to increase with increasing presence of target fluorophore. Mathematically the Double Ratio can be expressed as<sup>15</sup>:

$$\text{Double Ratio} \propto \frac{1 + \frac{H_{i,t}}{C_r A_{i,t}} C_t}{1 + \frac{H_{j,t}}{C_r A_{j,t}} C_t} = \frac{1 + a C_t}{1 + b C_t} \quad (2)$$

Where the constants A and H stand for the fluorescence yield of the reference- and target fluorophore, respectively, and the parameters  $C_r$  and  $C_t$  stand, for the concentration of the reference- and the target fluorophore, respectively. The parameters a and b are material constants and thus the Double Ratio varies with the amount of target fluorophore amount. Artifacts caused by absorption, scattering, variations in natural tissue fluorescence, excitation fluence and geometry are all cancelled out<sup>15</sup>. Later work revealed that the Double Ratio, besides 'target fluorophore' concentration, also has a dependency on the fluorescent layer thickness<sup>17</sup>. The relation between the Double Ratio and target fluorophore concentration  $C_t$  is described by eq. 2 and plotted in fig. 1. The initial slope of the curve equals a minus b and the curve approaches the asymptotic

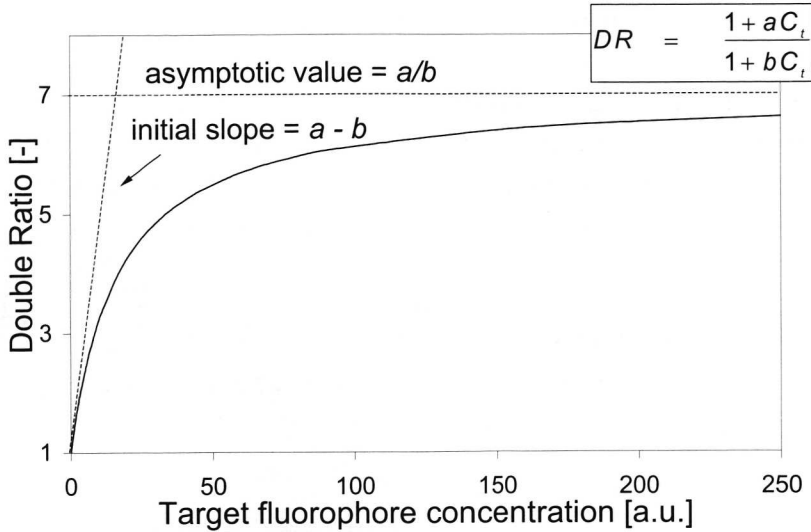


Figure 1: The relation between the Double Ratio and target fluorophore concentration ( $C_t$ ).

value of  $a/b$  for high target fluorophore concentrations. For maximum sensitivity to changes in amount of fluorophore the difference between  $a$  and  $b$  is preferably as large as possible. This can be obtained by choosing both excitation wavelengths to have a: 1.) maximum difference in fluorescence yield for the target fluorophore and, 2.) a minimum difference in fluorescence yield for the reference fluorophore, see Eq. 2. The Double Ratio measurement technique can be adapted for any kind of 'target fluorophore'. In principle the approach can also be employed for other types of spectroscopic techniques such as Raman scattering. Prerequisites are sufficiently different excitation spectra for the target and reference fluorophore, and the selection of appropriate excitation and detection wavelengths.

### Imaging system

A novel fluorescence imaging system has been developed and built, according to the Double Ratio technique. A diagram of the system is shown in fig.2. The output beam of a lamp (Ushio, 200W, XeHg) is split in two by a beam splitter. The two beams are separately guided through excitation filters, a chopper (EG&G, 651-1E) and focussed into two meter long liquid light guides with a core diameter of 8 mm for illumination of the target area. Fluorescence light from the target area is collected by a first lens. By exchanging the first lenses the camera magnification can be changed, with a focal length of 10cm or 30cm the detection area is either 1x1cm or 3x3cm. For the longest focal length the excitation power is in the range of a few hundred microWatts per square centimeter.

Excitation and detection filters as well as cameras can be changed easily. Fluorescence emitted from the tissue is detected through two detection filters, covering the vertical halves of the CCD chip. Dedicated optics focus four equal images on this single chip. A slave chopper (EG&G, 651-1E) in the camera unit is synchronized with the chopper in the lamp unit. The slave chopper alternates between the horizontal halves of the CCD. A

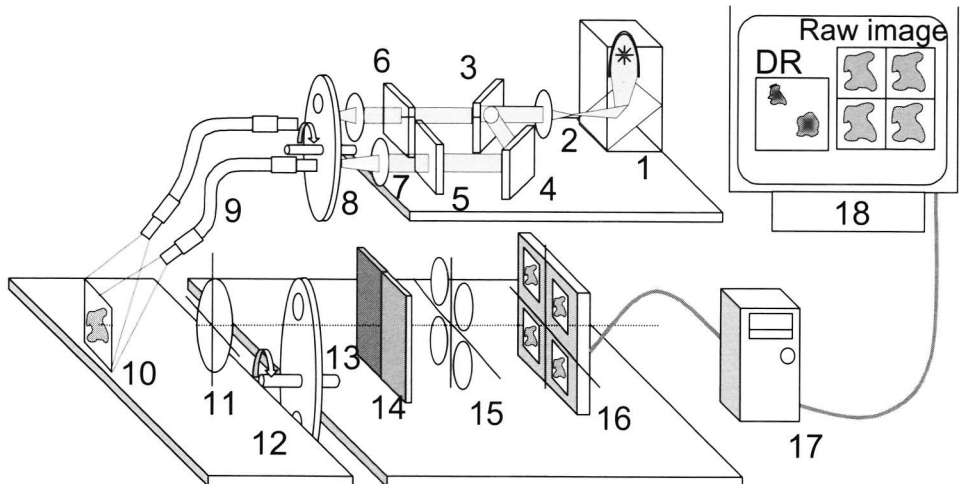


Figure 2: Overview of the Double Ratio imaging system which can acquire 4 fluorescence images excited at 2 wavelengths and detected at 2 wavelengths. Four images are focused on one CCD chip. Two wavelength detection is then realized by covering each half of the CCD with a filter. Two wavelength excitation is accomplished with an alternating light source. Excitation and image acquisition is synchronized with choppers. Excitation unit: 1.) 200W XeHg lamp, 2. Lens, 3. Beam splitter, 4. Mirror, 5. Excitation filter i, 6. Excitation filter j, 7. Lenses, 8. Chopper (master), 9. Liquid light guides. Detection unit: 10. Tissue, 11. First lens, 12. Chopper (slave), 13. Detection filter t, 14. Detection filter r, 15. Second lens, 16. CCD chip. Processing unit: 17. PC, 18. Display

figure of the illumination phases is shown in fig. 3. This prototype allows us to acquire four equal images excited at two wavelengths and detected at two wavelengths. The chopping frequency is chosen to be much higher than the frame rate of the camera i.e. a rate of 1200 Hz. This enables the camera to run with a frequency independent of the chopping procedure. In this way we are able to use a wide range of cameras. In our experiments two different types of cameras are used. A high speed slow scan 14 bit cooled monochrome CCD camera, Proscan HSS 1024, with 1024x1024 pixels and a PCI interface. The second camera is a Philips IP 800, a two step intensified video camera. At maximum gain this camera has a sensitivity of 5 $\mu$ lux. Interface is a Data translation DT3152 frame grabber. With dedicated software, Interactive Data Language (IDL), the four separate spectral images are extracted and Double Ratio images are calculated, exactly overlaying and dividing the 4 images pixel by pixel according to Eq. 2. Finally,

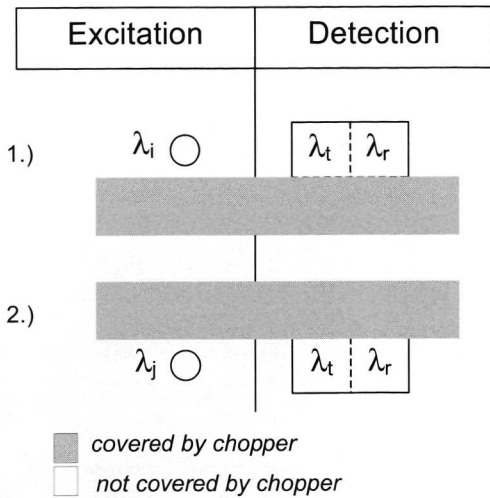


Figure 3: Acquisition of four equal images with two wavelength excitation and two wavelength detection is performed within 2 illumination phases of the CCD chip: 1.) A detection phase with excitation wavelength  $\lambda_i$ . Here two wavelength detection of  $F_{i,t}$  and  $F_{i,r}$  takes place on the upper half of the CCD through the reference ( $\lambda_r$ ) and target detection filter ( $\lambda_t$ ). 2.) A detection phase with excitation wavelength  $\lambda_j$ . Here a two wavelength detection of  $F_{j,r}$  and  $F_{j,t}$  takes place on the lower half of the CCD through the reference ( $\lambda_r$ ) and target ( $\lambda_t$ ) detection filter.

filters are:  $\lambda_i$ : 405nm, (Oriel 56541) and  $\lambda_j$ : 435nm, (Oriel 56551). Detection band pass filters for the 'reference fluorophore' are:  $\lambda_r$ : 550nm, (Omega optical 550RDF42) and for the 'target fluorophore'  $\lambda_t$ : 675nm, (Omega optical 675DF110), see fig. 2. To prevent any excitation light to enter the camera a long pass filter is positioned in front of the first lens (Schott KV500), not in fig. 2. A schematic representation of the Double Ratio calculation with these filters is shown in fig. 4.

### Tissue equivalent phantom study

Tissue equivalent phantom studies have been performed to investigate the sensitivity of the Double Ratio images to changes in the absorption coefficient  $\mu_a$  and scattering coefficient  $\mu_s$ . Aqueous solutions were prepared with varying concentrations Intralipid 10% as a scattering component and Evans Blue as the absorbing component. To simulate natural tissue fluorescence we used Fluorescein as 'reference fluorophore'.

Hematoporphyrin (Hp) was used as 'target fluorophore'. Before adding Hp to the phantom it was pre-diluted in a small amount of acetone to enhance solubility in water.

Double Ratio images are displayed at a maximum speed of 1Hz. This system allows to image a wide variety of fluorophores and different tissue types. In practical use the system resembles an operating microscope and can be used in a clinical environment.

### Experiments

In theory Double Ratio values are independent of tissue optics, i.e. the scattering coefficient ( $\mu_s$ ) and absorption coefficient ( $\mu_a$ ). To check whether our prototype functions accordingly we performed two experiments: 1.) An *ex vivo* tissue equivalent phantom study and, 2.) an *in vivo* study of normal human pigmented moles on normal Caucasian skin. For these 2 experiments we used porphyrins as 'target' fluorophore. The chosen excitation wavelengths band pass

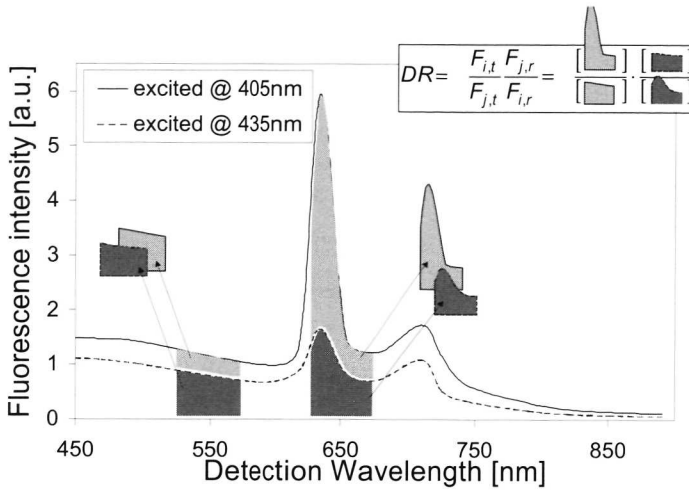


Figure 4: Graphic presentation of the fluorescence signals needed to calculate a Double ratio. Shown are two schematic fluorescence spectra of tissue with porphyrin. One spectrum is excited at 405nm and the other is excited at 435nm. The grey areas indicate the fluorescence signals in the appropriate wavelength bands needed to calculate a Double Ratio.

Five different phantoms were made in total. The range of optical properties that were used is listed in table 1. Double Ratio imaging took place for each phantom while varying the Hp concentration.

### Human mole study

Previous studies have shown that high absorption of dark colored lesions on a less absorbing light colored skin can cause biased fluorescence measurements<sup>14</sup>. To study how our prototype deals with these absorption artifacts in vivo we studied normal pig-

Table 1: The optical properties of the tissue equivalent phantoms at 635nm. Phantom 4 aims to simulate human epidermis, while phantom 5 aims to simulate human liver<sup>18</sup>.

Phantom	$\mu_s$ [ $\text{cm}^{-1}$ ]	$\mu_a$ [ $\text{cm}^{-1}$ ]
1	80	2.8
2	120	2.8
3	80	4.2
4	244	1.8
5	313	2.3

mented moles on Caucasian skin, comparing the Single Ratio introduced by Profio to correct for background fluorescence<sup>12</sup> with Double Ratios.

Here, the Single Ratio is the protoporphyrin IX fluorescence detected in the red (675nm), divided by the natural tissue fluorescence, detected in the green (550nm), both excited at 405nm. The measurements were performed on two volunteers on which we selected two pigmented moles each. Topical administration with a solution

of 20% ALA in Instillagel took place. The gel was applied on the pigmented mole and surrounding light colored skin and was held into position with Tegaderm. Through metabolic reactions in the tissue ALA is converted to the 'target fluorophore' Protoporphyrin IX. After half an hour the Tegaderm was removed and the skin was cleaned with a gauze. Two hours later Double Ratio images were taken.

## Results

### Tissue equivalent phantom study

Fig. 5 shows the Double Ratio values versus Hp concentration for the five phantoms. The graph shows five similar measured curves close to curve predicted by eq. 2. There is a good correlation between the measured values and the theoretically predicted curve given by Eq. 2, which is plotted in the graph as well. A correlation coefficient of 0.98 was found.

### Human mole study

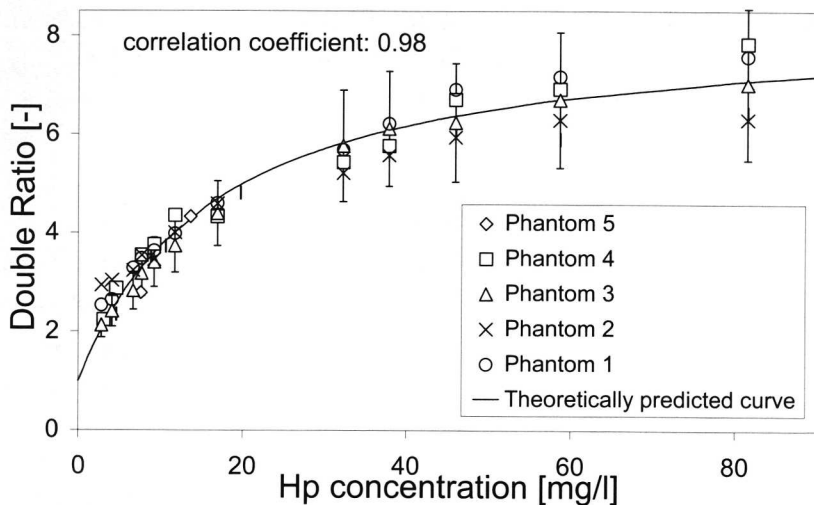


Figure 5: Hp concentration versus Double Ratio for five different phantoms (see Table 1.). Although these phantoms have different absorbing and scattering properties similar Double Ratio values were found close to the curve predicted by Eq. 2. A correlation coefficient of 0.98 was calculated between theory and measurement.

Fig. 6a shows natural tissue fluorescence image of a clinically benign pigmented mole on normal light colored skin at 550nm. Throughout the whole image hairs are visible and a v-mark was drawn on the skin for easy recognition of the lesion. Obvious are the higher absorption at the location of the mole and the marking. Figure 6b shows the protoporphyrin IX fluorescence divided by the natural tissue fluorescence ratio of the same

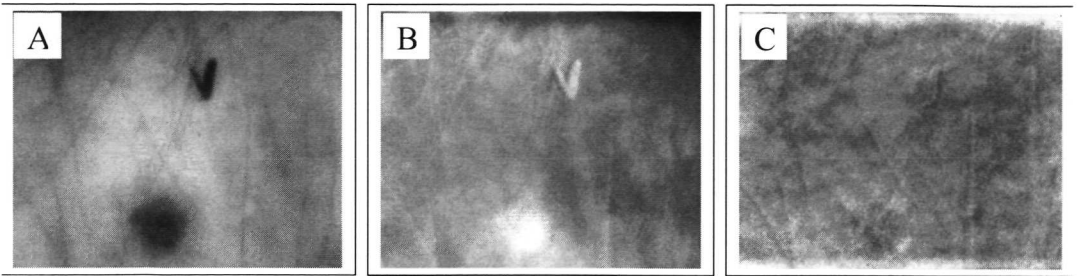


Figure 6: Fluorescence images of a normal dark colored mole on a normal light colored skin after application of 5-ALA. We drew a v-mark on the skin for easy recognition. Left: Natural tissue fluorescence image (550nm). Middle: protoporphyrin IX fluorescence image (675nm) divided by the natural fluorescence ratio image (550nm) here we see biased elevated values at the position of the v-mark and mole due to a stronger absorption in the green in comparison with the red. Right: Double ratio image with similar values for mole, v-mark and skin, indicating similar protoporphyrin IX levels for mole, v-mark and surrounding skin mole. The normal lesion and v-mark show a clearly higher ratio in comparison with the normal surrounding tissue, illustrating the fact that green light is absorbed stronger than red light in this mole and v-mark, which biases this ratio. Fig. 6c shows the Double Ratio image. Both the normal mole and v-mark have disappeared which is an indication that they have similar porphyrin concentrations in comparison with the surrounding tissue. The v-mark and hairs have not completely disappeared but are still slightly visible. This may be caused by non exact overlay of the four images. We found similar results in all 4 moles.

## Conclusions

We have designed and constructed a fluorescence imaging system for the detection of superficial cancers. This system can acquire, display and store Double Ratio images. Typical acquisition time of a Double Ratio image is within the range of a second, using an image intensified camera and a minute using a slow scan cooled CCD. In practical use this system resembles an operating microscope and can be used in a clinical environment. By exchanging the optics the detectable area is either 3x3cm or 1x1cm with a focal length of 10cm or 30cm, respectively. Currently the system is configured to measure Protoporphyrin IX (PpIX) fluorescence. By exchanging the excitation and detection filters any fluorophore of choice can be investigated.

Our Double Ratio fluorescence imaging device was capable of localizing porphyrin concentrations independent of tissue color, tissue phantom color and tissue phantom scattering. Due to these useful properties Double Ratio fluorescence imaging may provide additional diagnostic information in comparison with currently available fluorescence imaging systems. Hence, Double Ratio imaging may serve as an additional tool for the

clinical detection of cancers and its precursors. Clinical studies with this device are underway.

## **Acknowledgements**

This work was funded by "The Dutch Technology Foundation", grant no. AGN 44.3413, and the European Commission, BIOMED, grant no. BMH4 CT172260

We also acknowledge the mechanical engineering efforts of Arie Steenbeek.

## References

1. G.A.Wagnieres, W.M. Star, B.C. Wilson, In vivo fluorescence spectroscopy and imaging for oncological applications. *Photochem. Photobiol.*, 1998, **68**, 603-632.
2. S. Andersson-Engels, J. Johansson, K. Svanberg, S. Svanberg, Fluorescence imaging and point measurements of tissue: applications to the demarcation of malignant tumors and atherosclerotic lesions from normal tissue. *Photochem. Photobiol.*, 1991, **53**, 807-814.
3. M. Kriegmair, D. Zaak, H. Stepp, R. Baumgartner, R. Knuechel, Transurethral resection and surveillance of bladder cancer supported by 5-aminolevulinic acid-induced fluorescence endoscopy, *Eur. Urol.* 1999, **36(5)**, 386-392.
4. W. Stummer, A. Novotny, H. Stepp, C. Goetz, K. Bise, Fluorescence-guided resection of glioblastoma multiforme by using 5-aminolevulinic acid-induced porphyrins: a prospective study in 52 consecutive patients. *J. Neurosurg.*, 2000, **93(6)**, 1003-1013.
5. P. Hillemanns, H. Weingandt, R. Baumgartner, J. Diebold, W. Xiang, H. Stepp. Photodetection of cervical intraepithelial neoplasia using 5-aminolevulinic acid-induced porphyrin fluorescence. *Cancer* 2000, **88(10)**, 2275-2282.
6. S. Lam, B. Palcic. Autofluorescence bronchoscopy in the detection of squamous metaplasia and dysplasia in current and former smokers. *J. Nat. Cancer. Inst.*, 1999, **91**, 561-563.
7. R.S. DaCosta, B.C. Wilson, N.E. Marcon, Light-induced fluorescence endoscopy of the gastrointestinal tract. *Gastrointest Endosc Clin N Am* 2000, **10(1)**, 37-69, vi.
8. M. Zargi, I. Fajdiga, L. Smid. Autofluorescence imaging in the diagnosis of laryngeal cancer. *Eur Arch Otorhinolaryngol* 2000, **257(1)**, 17-23.
9. S. Lam, C. MacAulay, J. Hung, J.C. Leriche, A.E. Profio, B. Palcic. Detection of dysplasia and carcinoma in situ with a lung imaging fluorescence endoscope device. *J. Thor. Cardiovasc. Surg.*, 1993 1035-1040.
10. R. Baumgartner, H. Stepp. Photodynamic diagnosis using 5-aminolevulinic acid (5-ALA) for minimally-invasive treatment of cancer. *Min. Invas. Ther Allied. Technol.* 1998, **7(6)**, 495-501.
11. R. Baumgartner, H. Fisslinger, D. Jocham, H. Lenz, L. Ruprecht, H. Stepp A fluorescence imaging device for endoscopic detection of early stage cancer - instrumental and experimental studies. *Photochem. Photobiol.*, 1987, **46**, 759-763.
12. A.E. Profio, O.J. Balchum, F. Carstens., Digital background subtraction for fluorescence imaging. *Med. Phys.*, 1986, **13**, 717-721.
13. S. Andersson-Engels, J. Ankerst, J. Johansson, K. Svanberg, S. Svanberg. Laser-induced fluorescence in malignant and normal tissue of rats injected with benzoporphyrin derivative. *Photochem. Photobiol.* 1993 **57(6)**, 978-983.
14. H.J.C.M. Sterenborg, A.E. Saarnak, R.G.J. Frank, M. Motamedi., Evaluation of spectroscopic correction techniques for in vivo fluorescence measurements on pigmented lesions. *J. Photochem. Photobiol.*, 1996, **B35**:159-165.
15. M. Sinaasappel, H.J.C.M. Sterenborg. Quantification of hematoporphyrin derivative by fluorescence measurement using dual wavelength excitation and dual wavelength detection. *Appl. Opt.* 1993, **32**, 541-548.

16. A.E. Saarnak, T. Rodrigues, J. Schwartz, A.L. Moore, M.J.C. van Gemert, Thomsen S, Influence of tumor depth, blood absorption and autofluorescence on measurement of exogenous fluorophores in tissue. *Las. Med. Sci.*, 1998, **13**, 22-31.
17. W.F. Cheong, A. Pahl, A.J. Welch. A review of the Optical Properties of Biological Tissues. *IEEE J Quant Electr* 1990, **26(12)**, 2166-2185.

